ARTICLE OPEN

Check for updates

Maternal prenatal stress induces sex-dependent changes in tRNA fragment families and cholinergic pathways in newborns

Shani Vaknine Treidel[1,2], Silvia M. Lobmaier[3], Ritika Sharma[3,4], Nimrod Madrer[1], Serafima Dubnov[1], Dana Shulman[1], Pnina Greenberg[1], Estelle R. Bennett[1], David S. Greenberg[1], Adi Turjeman[5], Camilla Zelgert[3], Peter Zimmermann[3], Martin G. Frasch[6], Liran Carmel[2], Marta C. Antonelli[3,7] and Hermona Soreq[1]✉

Maternal perceived prenatal stress (PPS) is a known risk factor for diverse developmental impairments in newborns, but the underlying molecular processes are incompletely understood. Here, we report that maternal PPS altered the birth profiles of blood transfer RNA fragments (tRFs), 16–50 nt long non-random cleavage products of tRNAs, in a sex-dependent manner. Importantly, comparing stressed versus control maternal and umbilical cord blood serum presented alterations that were not limited to individual tRFs, but rather reflected selective changes in particular tRF families grouped by their mitochondrial or nuclear genome origin, parental tRNA coded amino acid, and cleavage type. Specifically, tRF families that show stress- and sex-specific effects, revealed shared length and expression patterns which were strongest in the female newborns. Several of these tRFs carry complementary motifs to particular cholinergic mRNAs, suggesting possible translational regulation similar to microRNAs. Compatible with the cholinergic regulation of stress reactions, those "CholinotRFs" achieved an AUC of 95% when classifying female newborns according to maternal PPS. Moreover, we found altered catalytic activity of serum acetylcholinesterase, which was particularly elevated in male newborns, marking a second sex-specific effect. Our findings demonstrate an association of tRF families' patterns with newborns' sex-specific stress response to PPS and may lead to better diagnosis and therapeutic tools for these and other stressors.

Molecular Psychiatry; https://doi.org/10.1038/s41380-025-03011-2

INTRODUCTION

The womb environment plays a crucial role in determining the future physical and mental health of the fetus, through the effects of numerous factors affecting fetal development [1–3]. Specifically, psychosocial stress expressed as clinical or preclinical prenatal depression or anxiety affects 20% of all pregnancies [4–6]. While direct measurements of psychological stress are subjective in nature, perceived stress measurement offers a valuable alternative [6, 7]. Indeed, prenatal perceived stress (PPS) associated with offspring neurodevelopmental impairments, including neurobehavioral problems and greater vulnerability to later psychiatric disorders [8, 9]. Moreover, PPS negatively correlates with fetal left hippocampal volume [10, 11], infant cognitive performance at 18 months [4], and newborn telomeres length [12, 13]. Some of these effects are sex-specific, showing male newborns as more vulnerable [5, 14]. Proposed mechanisms mediating these effects include epigenetic programing [15] and maternal immune activation through the hypothalamic-pituitary-adrenal axis (HPA), although cortisol-mediated fetal programming presented conflicting evidence [6, 16, 17]. However, the role of short noncoding RNAs in these processes remained unknown.

tRNA fragments (tRFs) are 16–50 nucleotides long noncoding RNAs which are highly conserved across the evolutionary tree and are cleaved from pre- and mature tRNAs by specific endonucleases [18, 19]. Human tRNA genes originate from both the nuclear and the mitochondrial (MT) genomes, and both are important for healthy cell function [20]. Moreover, the nuclear genome contains "lookalike" tRNA genes, mimicking MT tRNAs, hailing their functional importance also outside the mitochondria [21]. The more widely studied tRFs are cleaved from mature tRNAs, and are classified into five groups based on their cleavage point: 5′-half and 3′-half tRFs are produced by angiogenin cleavage at the anticodon loop, splitting the tRNA into two halves, whereas 5′-tRFs, i-tRFs, and 3′-tRFs are cleaved around the D- and T-loops by a combination of angiogenin, dicer and other endonucleases, splitting the tRNA into three parts [20, 22]. Interestingly, these cleavage points are not precise and can vary in length across tRFs sharing their cleavage type [20], sometime influenced by pre-existing tRNA modifications, such as methylation and pseudouridylation, which are actively involved in the biogenesis of tRFs [19, 23]. Further, tRFs can regulate transcription and translation by various mechanisms, including complementary binding to other

[1]Department of Biological Chemistry and the Edmond and Lily Safra Center of Brain Science, the Hebrew University of Jerusalem, Jerusalem, Israel. [2]Department of Genetics, the Hebrew University of Jerusalem, Jerusalem, Israel. [3]Department of Obstetrics and Gynecology, Technical University of Munich, Munich, Germany. [4]Helmholtz Centre Munich, German Research Center for Health and Environment (GmbH), Munich, Germany. [5]Genomic Center, the Hebrew University of Jerusalem, Jerusalem, Israel. [6]Department of Obstetrics and Gynecology and Institute on Human Development and Disability (IHDD), University of Washington, Seattle, WA, USA. [7]Instituto de Biología Celular y Neurociencias "Prof. E. De Robertis", Facultad De Medicina, UBA, Buenos Aires, Argentina. ✉email: hermona.soreq@mail.huji.ac.il

Received: 18 August 2024 Revised: 5 March 2025 Accepted: 31 March 2025
Published online: 05 April 2025

RNAs or RNA binding proteins, promotion of ribosome biogenesis, and post-transcriptional gene silencing via the RISC complex [19, 22–24]. The roles of tRFs have been explored in neurodegenerative diseases, cancers, stroke and non-alcoholic fatty liver disease [23, 25–28], but their impact on pregnancy complications or developmental disorders was only scarcely studied [29, 30].

The cholinergic system controls cognitive processes, inflammatory events, and neuromuscular communication [31–34] and is a major regulator of stress responses, which play an active role in trauma reactions, neurodegeneration, stroke and other mental conditions [35, 36]. As a major player in both the central and the peripheral nervous system, acetylcholine is produced in neurons as well as in liver and immune cells and is hydrolyzed by two cholinesterase enzymes. The major cholinesterase in the brain is acetylcholinesterase (AChE) and in the periphery, butyrylcholinesterase (BChE) [31, 32]. AChE can also be found on the membrane of erythrocytes in adult blood [37], in the placenta and in umbilical cord endothelial cells in the fetus [38, 39]. Altered balance between the circulation activities of these two enzymes reflects different conditions, from anxiety to Alzheimer's disease [35]. Cholinesterases and other cholinergic genes are regulated in several psychological disorders by "CholinomiRs" [40], microRNAs (miRs) carrying complementary sequences to those of cholinergic genes that enable them to suppress their expression [32, 37, 41]. Interestingly, certain tRFs may likewise regulate cholinergic genes via similar mechanisms. Importantly, circulating "CholinotRF" levels are elevated while CholinomiR levels decline in nucleated blood cells from post-ischemic stroke survivors [27], and mitochondrial-originated CholinotRFs show sex-specific cognition-related declines in the nucleus accumbens of women living with Alzheimer's disease [25].

Based on these and other studies, we explored fetal reactions to PPS as part of the 'FELICITy' study collection, under the hypothesis that CholinotRFs may present a promising avenue to study newborns reactions to PPS [42–45]. This unique cohort spanned a comprehensive battery of biomarkers in 120 mother-baby dyads, aiming to identify the stressed newborns at the earliest possible stage. Previous studies yielded a list of biomarkers: the fetal stress index (FSI), measuring fetal heart rate reaction to fluctuations in the maternal heart rate during the third trimester; maternal hair cortisol levels at birth [45]; umbilical cord serum (UCS) iron homeostasis markers [44]; and DNA methylation in newborns' saliva [43]. All of these biomarkers presented differences between stress and control groups, some in a sex-specific manner, e.g., transferrin saturation levels which were changed only in male newborns in the PPS group [44].

Our in-depth exploration of the impact of PPS on the newborn reflects maternal PPS assessed during the third trimester by profiling modulated tRFs levels and catalytically active cholinesterase enzymes in mothers and offspring at birth, as the earliest indicators of newborns' reaction to PPS. These analyses identified sex-specific differences both in particular tRF families and in cholinesterase activities, which differentiated between newborns of stressed and non-stressed mothers. Importantly, our analysis pipeline showed that grouping tRFs into families based on shared properties was more informative than considering each tRF type separately and that CholinotRFs enabled accurate PPS-based classification of female newborns.

MATERIALS AND METHODS

Participant recruitments and sample collection

A cohort of 18–45 years old women with singleton pregnancies were recruited (July 2016–May 2018) by the Department of Obstetrics and Gynecology at Klinikum Rechts der Isar Hospital of the Technical University of Munich, as part of the FELICITy project [44, 45] (Supplementary Methods). PPS was assessed during their early third trimester using the Cohen Perceived Stress Scale (PSS-10) questionnaire [7]. Based on a pilot study, women who achieved PSS < 19 were assigned to the control group and those with PSS ≥ 19 to the PPS group [45]. The women also completed the prenatal distress questionnaire (PDQ) [46] assessing pregnancy-related stress, which was highly correlated with PSS-10 scores (Supplementary Fig. 1c). 728 women completed the PSS-10, and at the day of the birth venous maternal blood was collected from 128 of them upon entry into the delivery room. Umbilical cord blood (arterial or venous) was collected from 120 of the matched newborns post-partum. All blood samples were collected into 9 mL S-Monovette® Serum Gel with Clotting Activator tubes (Sarstedt, # 02.1388). Serum was separated by a 10 min centrifugation at 2500 RPM, frozen at −20 °C and kept long-term at −80 °C. Samples were shipped on dry ice to the Hebrew University of Jerusalem Soreq lab, where they were kept at −80 °C until analysis.

Cholinesterase activity measurements

Serum cholinesterase activity was measured using Ellman's assay [47], in samples from 70 mothers and newborns who experienced non-emergency vaginal birth. Briefly, samples were diluted 1:20 in phosphate buffered saline and mixed with Ellman's solution in 96 flat-well plates. Samples were incubated under three conditions: without inhibitors, with the BChE inhibitor tetraisopropylpyrophosphoramide (iso-OMPA; final concentration 50 µM; Sigma, T1505), and with the AChE inhibitor BW284c51 (final concentration 5 µM; Sigma, A9103). Absorbance was read at 436 nm in a Tecan Spark™ 10 M plate reader (Tecan Group, Switzerland) for 21 kinetic cycles of one minute each. Measurements were analyzed using R [48]. See Supplementary Methods for more details.

Serum RNA extraction

Short RNA was extracted from both maternal and newborn serum samples using the miRNeasy Serum/Plasma Advanced Kit (Qiagen, 217204) according to manufacturer's instructions, including the additional centrifugation step after defrosting the samples and before starting the protocol. Concentration measurements (NanoDrop 2000, Thermo Scientific) showed average yields of 14.3 ng/µL. Quality assessment (Bioanalyzer 6000, Agilent) showed average RIN values of 1.8, reflecting the almost complete lack of rRNA in serum [49] rather than poor quality.

Sequencing and alignment

Of the 120 UCS samples, only those of dyads of mothers scoring either low (PSS-10 ≤ 10) or high (PSS-10 ≥ 19) PPS were considered for short RNA sequencing (Supplementary Fig. 1a). Samples were divided into four groups by the mothers' PSS-10 score and the newborn sex, and for each group the 12 samples with highest RNA concentration in NanoDrop and Bioanalyzer assessments were sequenced (n = 48). To avoid birth types confounding the sequencing results, we only analyzed 35 RNA samples of non-emergency vaginal births (Supplementary Fig. 1b); divided into four groups: female and male newborns from PPS mothers (female stress, n = 6; male stress, n = 8) and female and male newborns from control mothers (female control, n = 11; male control, n = 10). A subset of 24 samples from mothers corresponding to the sequenced newborns was chosen to form matched dyads (n = 6 in all four groups), based on the highest RNA concentration in the maternal cohort. Average RNA yields of sequenced samples were 21.4 ng/µL.

Libraries were constructed using the D-Plex Small RNA-seq Kit for Illumina (Diagenode, C05030001) and short RNA was sequenced on the NextSeq 500 System (Illumina) at the Center for Genomic Technologies, the Hebrew University of Jerusalem. Newborn and maternal samples were size-selected for 70–80 nt (Supplementary Methods) and sequenced on separate flow cells (NextSeq 500/550 High Output Kit v2.5 75 Cycles, Illumina, 20024906) using 1600 pg/sample in the newborn cohort and, due to lower RNA yield, 400 pg/sample in the maternal one. Consequently, the sequencing depth was ~16 M reads for newborns and ~18 M for maternal samples, the lower concentration of the maternal samples resulting in more availability of reads per sample. Subsequent quality control was re-assessed using FastQC [50] version 0.11.8, with Cutadapt [51] for removing the adaptor sequences, followed by Flexbar [52, 53] for further quality screening and cleaning. Alignment to tRFs was done using MINTmap [54] to MINTbase v2.0 [55] and to microRNA using miRDeep2 [56] to miRbase 22.1 [57, 58]. MINTbase accessions were converted to "tDR" names using the tDRnamer algorithm [59], with a few exceptions detailed in the Supplementary Methods.

Statistical analysis

Differential expression analysis. Differential expression analysis was performed using the DESeq2 [60] package in R with their suggested prefiltering step, disqualifying all miRs and tRFs that did not achieve rowSums(counts(dds) >= 10) >= smallestGroupSize, where smallestGroupSize = 6. This left 565 and 174 tRFs and 69 and 49 miRs for downstream analyses in newborn and maternal samples, respectively. Normalized DESeq2 findings were deemed statistically significant for $p \leq 0.05$ after FDR correction using Wald's test. Analyses at the tRF family level, including length analysis, are detailed in the Supplementary Methods.

Identifying cholinergic targets. To identify miRs and tRFs that target genes in the cholinergic network we combined the miRDB sequence-based prediction algorithm [61, 62] with a modified version of our in-house cholinergic scoring system [25–27]. Briefly, we tested miRs and tRFs that were 17–28 nucleotides long who had targets with a prediction score ≥ 80, which were then matched against a list of 102 cholinergic genes (Supplementary Table 1). Those were assigned scores of one or five according to their role in the cholinergic network, with core genes (e.g. CHAT, ACHE) receiving a score of five and others (e.g. IL6, CHKB) receiving a score of one. For each miR/tRF a "cholinergic score" was calculated by summing the scores of their gene targets, thus identifying as CholinomiRs/CholinotRFs miRs or tRFs targeting (a) at least one core cholinergic gene and/or (b) at least five peripheral cholinergic genes.

Classification and visualization. SVM kernel classification was employed using the Caret R package [63] with a "leave-one-out" cross validation method, and the MLeval R package [64] served to calculate receiver operating characteristic (ROC) curve, area under the curve (AUC), accuracy, precision, F1 and recall values (Supplementary Table 8). P-values and subsequent false discovery rate (FDR) were calculated based on 10,000 permutations for five of the top marker groups (Supplementary Table 9).

RESULTS

Newborns of PPS-mothers show elevated serum AChE levels

To study whether maternal PPS scores can affect their cholinergic status and influence their newborns' reaction to the stress of birth, we measured serum acetylcholine hydrolyzing cholinesterase (ChE) activities in both mothers and newborns of the FELICITy cohort [42–45]. We classified mothers according to their third trimester perceived stress assessment by the PSS-10 questionnaire [7], which were predictably highly correlated with their PDQ values [46] (Supplementary Fig. 1c). Other cohort demographic or medical features did not differ significantly between the stress and control groups (Fig. 1b, Supplementary Fig. 1d). ChE activities in mothers' serum were similar between the stress and control groups, possibly due to sampling timing – upon entry to the delivery room (Fig. 2d), in line with previous results showing no significant difference in erythrocyte-bound AChE between pregnant women after membrane rapture and their non-pregnant healthy counterparts [65]. However, newborns UCS was sampled after birth, and indeed, newborns of stressed mothers showed higher serum AChE activities than those of control mothers, with male newborns showing generally higher AChE activity compared to female newborns (Fig. 2d; Mann–Whitney U test: Female P-value = 0.035, male P-value = 0.0048). Although not statistically significant, butyrylcholinesterase (BChE) activity in newborns showed the same trend (Fig. 2d), together suggesting altered serum acetylcholine levels in stressed compared to control newborns.

Interestingly, serum AChE activities in all newborn groups but female controls were higher compared to their mothers (Fig. 2e; Wilcoxon signed rank test, FDR ≤ 0.05; Supplementary Table 2), even when combining stress and control groups and testing all female and all male newborns compared to their mothers (female FDR = 2.9E-03, male FDR = 2.8E-04). This effect may be attributed to the additional sources of AChE in the umbilical cord blood and the placenta [38, 39], however, this did not explain the differences between newborn/mother AChE activities in the female control group.

Notably, AChE activity ratio was higher in stressed compared to control males (Mann–Whitney U test, P-value = 0.0072) and in stressed females compared to stressed males (P-value = 0.0087). BChE ratio presented a similar trend in the male stress group alone, showing higher BChE activity compared to their mothers (Fig. 2e; P-value = 0.041; Supplementary Table 2). In accordance with the anti-inflammatory effect of AChE [32], levels of immune marker transcripts in newborns showed sex-specific elevations (Supplementary Results and Supplementary Fig. 2). Hence, our findings identified higher AChE catalytic activity at birth indicating that newborns' may respond to their mothers' PPS via the cholinergic system at birth, and that male newborns show a stronger form of this reaction.

Serum miRs present small changes in newborns and mothers

Altered miRs and tRFs levels could suppress cholinesterase activities, therefore a decline in targeting miR/tRF can explain the observed elevations in AChE and BChE levels. Therefore, we compared serum miRs profiles between the newborns' stress and control groups (Fig. 3a–c). When combining male and female data, a stress-related decline in hsa-miR-301a-3p emerged (Fig. 3b), predicted to control autoimmune cell differentiation through regulating STAT3 in multiple sclerosis patients [66]. A parallel trend, albeit not significant, emerged in males and females studied separately (Fig. 3a, c). Male newborns of PPS mothers further showed elevated hsa-miR-7704 levels (Fig. 3a), which was also elevated in schizophrenia patients and may predict altered synapse activities [67]. Interestingly, previous pursuit of this cohort identified one hypo-methylated CpG, cg05306225 in newborns saliva [43] that was annotated to the schizophrenia-related CSMD1 gene [68, 69]. Two additional miRs, the hematopoietic regulating hsa-miR-223-3p [70, 71] and hsa-miR-142-5p [72, 73] showed declined levels in PPS mothers of female newborns alone (Supplementary Fig. 3c). Moreover, 30 of the detected miRs were expressed in both mothers and newborns, including hsa-miR-223-3p and hsa-miR-142-5p; however, hsa-miR-7704 and hsa-miR-301a-3p were unique to the newborns' samples.

All four differentially expressed (DE) miRs were previously connected to the immune system and to regulating cell division in various cancers [74–81], with the two found in both UCS and maternal serum previously connected to pregnancies. hsa-miR-223-3p is highly expressed in plasma exosomes of 30 and 38 weeks normotensive pregnant women and was suggested to be one of the controllers of the fetal–maternal immune balance [82]. Also, hsa-miR-142-5p levels in serum of mothers whose fetuses presented fetal congenital diaphragmatic hernia differ from control mothers at 26 weeks, 38–40 weeks, and 24 h after birth, and was suggested to cross between the fetal and maternal circulation [83]. These results emphasize the sex-specific effects of short noncoding RNAs, as evident in mothers of female newborns.

tRF families distinguish between stressed and control newborns, with a stronger effect in females

Unlike the small PPS-related miRs differences in serum, tRFs showed more pronounced patterns, starting with three DE tRFs separating stress and control newborn groups (Fig. 3e). Comparing the stress-by-sex groups revealed four DE tRFs separating female stressed newborns from controls (Fig. 3g), which are intriguingly distinct from the three tRFs identified when males and females were combined. All seven DE tRFs decreased in stressed newborns. Comparing male newborns alone failed to identify any DE tRFs (Fig. 3k).

Due to their shared genomic origin, parental tRNA coded amino acid, and cleavage type, diverse tRFs often present sequence similarity (Fig. 3d) [20], in contrast to miRs, and may hence share similar functions. Since tRFs are simultaneously produced from tRNAs by distinct nucleases [18, 19], we hypothesized that bulks of similar tRFs may be produced and function together, creating "tRF

a.

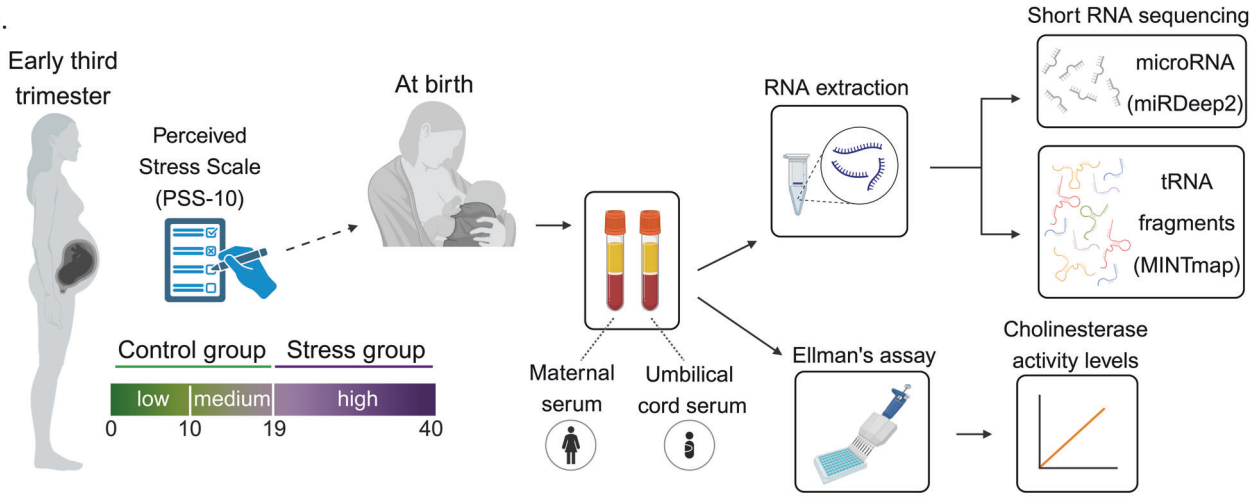

b.

Maternal psychological stress	Control (ctl)		Stress	
Newborns' sex	Female (N=19)	Male (N=23)	Female (N=14)	Male (N=14)
PSS score				
Mean (SD)	8.37 (4.07)	9.13 (3.79)	23.2 (3.12)	23.1 (3.61)
Median [Min, Max]	9.00 [1.00, 18.0]	10.0 [0, 15.0]	23.5 [19.0, 31.0]	22.0 [19.0, 32.0]
PDQ score				
Mean (SD)	8.89 (5.12)	7.26 (4.71)	15.8 (8.03)	15.6 (6.79)
Median [Min, Max]	9.00 [2.00, 20.0]	6.00 [3.00, 25.0]	16.5 [4.00, 35.0]	13.5 [8.00, 28.0]
Maternal age at study entry				
Mean (SD)	33.5 (3.47)	33.3 (3.25)	30.4 (5.02)	32.6 (4.16)
Median [Min, Max]	34.0 [28.0, 41.0]	33.0 [28.0, 39.0]	31.0 [21.0, 39.0]	31.5 [27.0, 38.0]
Maternal BMI at third trimester				
Mean (SD)	26.7 (2.58)	26.5 (3.45)	27.8 (4.42)	30.6 (5.60)
Median [Min, Max]	25.8 [23.0, 31.3]	26.2 [20.5, 37.3]	26.9 [21.2, 38.1]	28.8 [25.3, 43.2]
Maternal BMI before pregnancy				
Mean (SD)	21.9 (2.50)	22.0 (3.44)	23.1 (3.91)	25.5 (5.54)
Median [Min, Max]	21.0 [18.6, 27.4]	21.5 [18.2, 35.0]	22.4 [16.8, 31.9]	24.2 [20.0, 38.3]
Gestational age at birth (week)				
Mean (SD)	40.1 (1.12)	39.6 (1.05)	39.5 (0.909)	40.0 (1.01)
Median [Min, Max]	40.4 [37.7, 41.4]	39.6 [37.7, 41.7]	39.6 [37.7, 40.7]	40.1 [37.9, 41.4]
Number of births				
Mean (SD)	0.842 (0.765)	0.739 (0.752)	0.500 (0.519)	1.14 (1.29)
Median [Min, Max]	1.00 [0, 2.00]	1.00 [0, 2.00]	0.500 [0, 1.00]	1.00 [0, 4.00]
Apgar 5				
Mean (SD)	9.89 (0.315)	9.65 (0.714)	9.79 (0.579)	9.36 (0.745)
Median [Min, Max]	10.0 [9.00, 10.0]	10.0 [7.00, 10.0]	10.0 [8.00, 10.0]	9.50 [8.00, 10.0]
Newborn head circumference (cm)				
Mean (SD)	34.7 (0.632)	35.1 (1.46)	34.6 (1.29)	35.8 (1.46)
Median [Min, Max]	35.0 [34.0, 36.0]	35.5 [32.0, 38.0]	35.0 [32.0, 36.5]	35.5 [33.0, 38.0]
Newborn weight (gram)				
Mean (SD)	3520 (322)	3530 (376)	3430 (377)	3760 (438)
Median [Min, Max]	3530 [2880, 4150]	3540 [2960, 4490]	3410 [2680, 3950]	3820 [3020, 4490]

Fig. 1 Study layout and participant characteristics. a Mothers recruited early in the third trimester were assigned to psychosocial stress and control groups based on the Cohen Perceived Stress Scale 10 (PSS-10). Maternal blood samples (n = 128) were collected upon entry into the delivery room and umbilical cord blood samples (n = 120) were collected postpartum. Serum was extracted and served for ChE activity measurements and short RNA sequencing. Only mother-newborn dyads who had normal vaginal deliveries were used for subsequent analyses (Supplementary Fig. 1). **b** The four groups reflect combinations of maternal PPS scores and newborn sex. Maternal and newborn parameters pertinent to the study are presented with both mean and median. Created with BioRender.

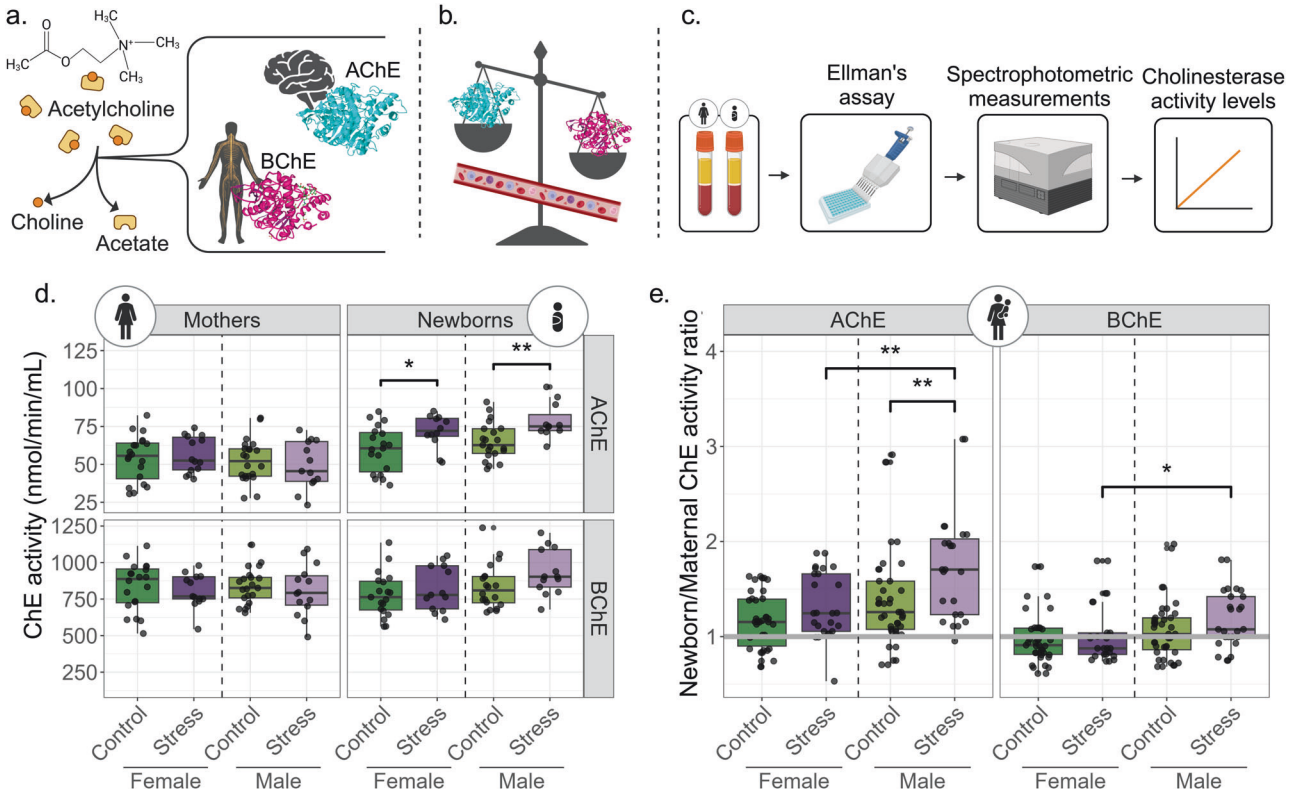

Fig. 2 Stressed newborns present altered ChE activities, reflecting cholinergic system involvement. a The cholinesterases AChE and BChE hydrolyze acetylcholine into acetate and choline. AChE is found predominantly in the brain and BChE in the periphery. **b** Balance between the two ChEs in the blood reflects different diseases and disorders. **c** Pipeline used to assess activities of ChEs in our cohort. **d** Boxplots comparing AChE and BChE activities in the serum of mothers and newborns (AChE: mothers, n = 69; newborns, n = 63. BChE: mothers, n = 68; newborns, n = 67). **e** Ratios between newborn and mother dyads for AChE (n = 62) and BChE (n = 64). The grey line indicates a ratio of one (equal ChE activities in mothers and newborns). P-values < 0.05, Mann–Whitney U test. IQR method to remove outliers was used in both d and e. Created with BioRender.

storms" [27]. If so, traditional DE analysis, which regards each tRF as an independent transcript, might fail to identify trends that would characterize whole "tRF families" whose joint biological impact may be considerable. To this end, we worked towards identifing tRF families that separate stressed and control male and female newborns (Fig. 3h–j, l–n). This revealed a profound decline in the levels of mitochondrial (MT) genome-originated tRFs in stressed female newborns, with 98.9% of the tRFs showing negative fold-change (Fig. 3h; exact binomial test FDR = 8.21E-74). Male newborns showed a similar, albeit less pronounced trend, with 90% of MT tRFs presenting negative fold-change (Fig. 3l; FDR = 9.06E-44). Declined 3′-tRFs levels were also apparent in both sexes (Fig. 3i, m; 73.6% in females, FDR = 3.38E-18; 74.5% in males, FDR = 1.73E-19), and in i-tRFs (65.5% in females, FDR = 7.66E-06; 59.6% in males, FDR = 0.0064). tRF families grouped by their coded amino acids showed varying trends too (Fig. 3j, n; Supplementary Table 3).

In contrast, the maternal cohort revealed no individual DE tRFs in any of those comparisons (Supplementary Fig. 3d, h, l). Yet, tRF family patterns in stressed mothers differed from those of the newborns, revealing a decline in nuclear genome-originated (Nuc) tRFs (Supplementary Fig. 3e; 71.1%, exact binomial test FDR = 2.1 E-03) and i-tRFs (Supplementary Fig. 3f; 80.9%, FDR = 4.5E-04), especially in mothers of male newborns (Supplementary Fig. 3m, n; Nuc: 64.5%, FDR = 4.6E-02; i-tRFs: 76.6%, FDR = 2.1E-03). Further, the maternal but not newborns cohort showed globally altered levels of tRF-halves (Supplementary Fig. 3f, j, n), with 3′-halves significantly elevated in all stressed mothers (87%, FDR = 2.2E-03), and in stressed mothers of male newborns separately (78.3%, FDR = 3.8E-02). Importantly, only 19 out of 45 tRF families in newborns and 30 in mothers were found in both cohorts. Moreover, the tRNA genes from which those tRFs were derived (according to the alignment by MINTmap) did not fully match the most prevalent tRNA genes, as shown by GtRNAdb [84, 85] for Nuclear-originated tRNA genes and by mitotRNAdb [86] for MT-originated tRNA genes (Supplementary Fig. 4a). Furthermore, tRF families with significantly modified trends did not necessarily coincide with the expected tRF families by MINTmap (Supplementary Fig. 4b). This phenomenon has been seen previously [23], although to the best of our knowledge was not studied directly, and adds to the notion that tRFs production is not random but may reflects a trend of tRF families to be produced together.

tRF families present distinct expression patterns in newborns and maternal serum

To further explore the hypothesis that specific tRF families function as groups based on their genome origin, parental tRNA coded amino acid and cleavage type, we sought shared stress-related changes in the levels of their members. Indeed, exact binomial test (FDR ≤ 0.05) identified 24 tRF families with significant DE values (Fig. 4b, Supplementary Table 3). Declined levels of MT-originated Gly-i-tRFs in stressed newborns (100% in stressed newborns and in stressed female alone, FDR = 3.5E-16 for both; 96.6% in stressed male newborns, FDR = 6.1E-13) revealed the strongest signal. The nuclear genome-originated Asp-i-tRFs were strongly elevated as well (83% in stressed newborns, FDR = 0.00009; 76.6% in stressed female, FDR = 0.0025; 76.6% in stressed male, FDR = 0.009). Mothers' tRF families presented no significant changes (Fig. 4b, Supplementary Table 4), however, comparing all stressed mothers to control mothers and mothers of

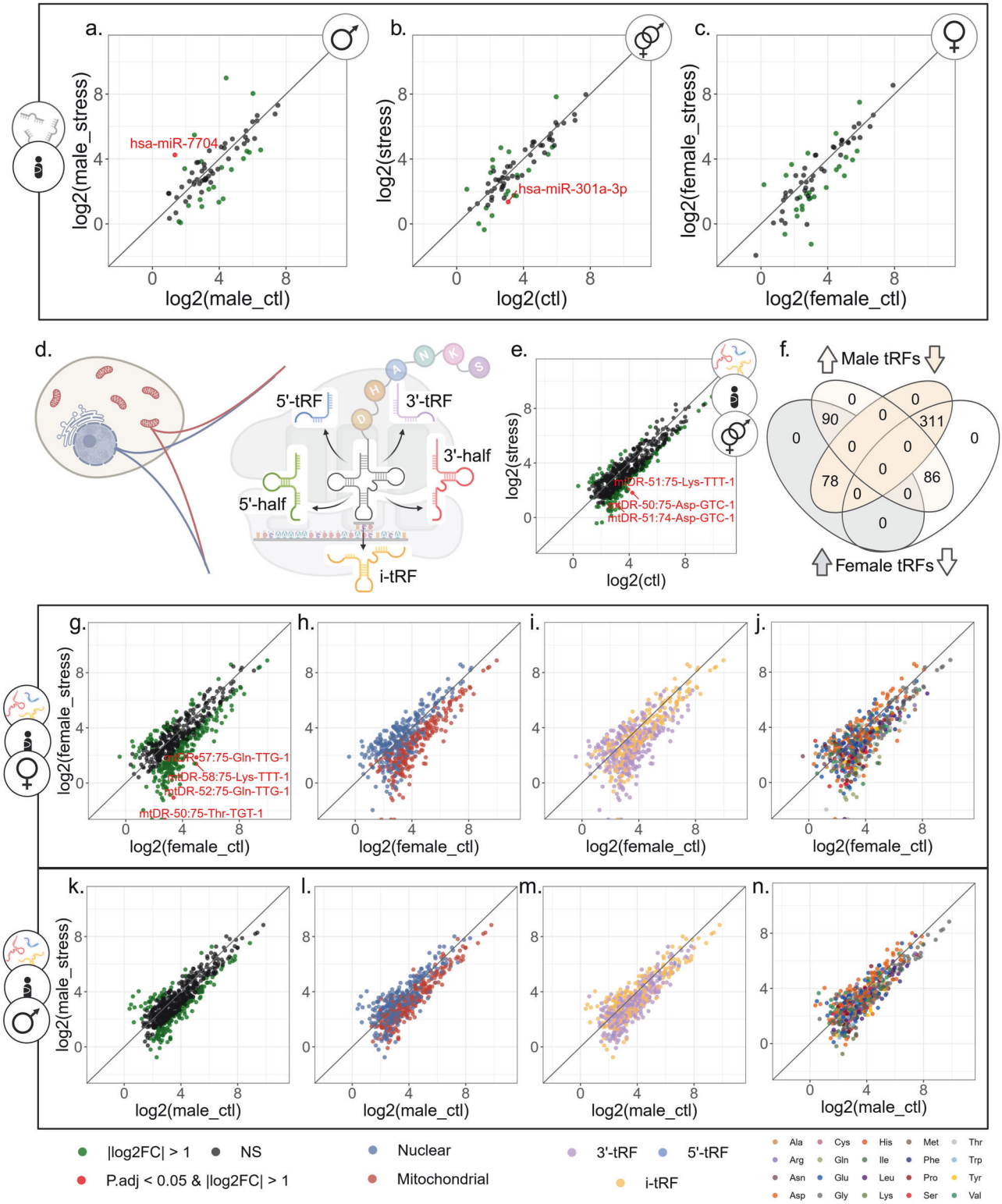

Fig. 3 tRF patterns differentiate stressed and control newborns, more than miRs. a–c Scatter plots of miR DE analysis in three contrasts: (**a**) stress vs. control male newborns (n = 8 vs. n = 10), (**b**) stressed vs. control male and female together (n = 14 vs. n = 21), and (**c**) in stress vs. control females (n = 6 vs. n = 11). X and Y axis representing the log2 of the average of counts of either stress or control group, accordingly. **d** tRNA genes are transcribed from two genome origins, nuclear (Nuc) and mitochondrial (MT), and encode specific amino acids. The mature tRNA is cleaved in specific locations, producing the five subtypes of tRFs: 5′-tRF, 5-half, i-tRF, 3′-half, and 3′-tRF. **e, g, k** Scatter plots of DE tRFs in (**e**) stressed vs. control male and female newborns together (n = 14 vs. n = 21), in (**g**) stress vs. control females (n = 6 vs. n = 11), and in (**k**) stress vs. control males (n = 8 vs. n = 10). **f** Venn diagram of overlapping tRFs with increasing and decreasing levels in the male and female comparisons. Scatter plots with tRFs colored according to genomic origin (**h, l**), cleavage type (**i, m**), (**j, n**) and tRNA coded amino acid **j, n**). Created with BioRender.

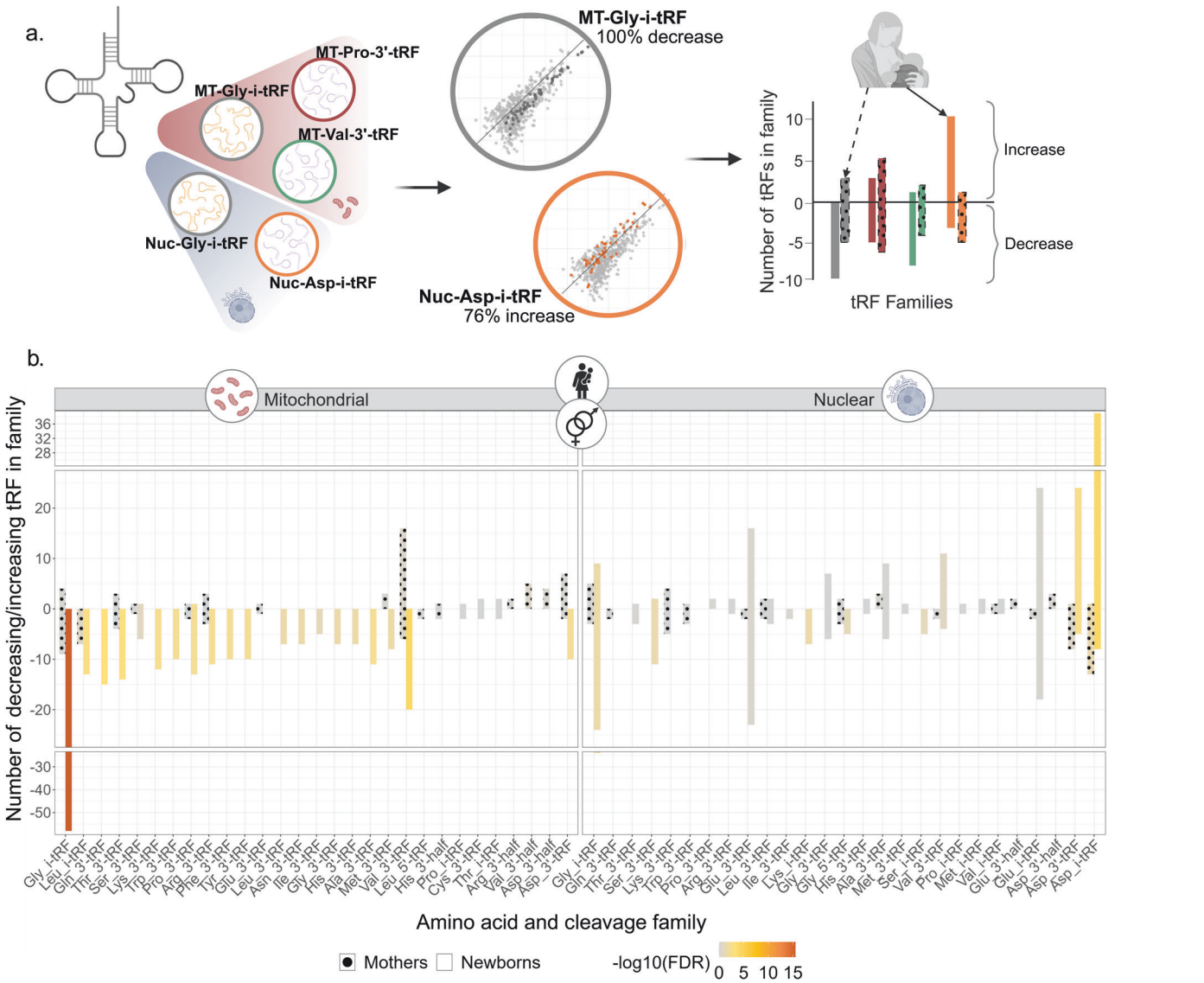

Fig. 4 tRF families differ significantly between stressed and control groups, with some inverse effects between mothers and newborns. **a** tRF families were defined based on their genome origin, cleavage type, and parental tRNA coded amino acid. Only families with one or more members were included in the analysis. The Exact Binomial test (FDR ≤ 0.05) was used to quantify the tendency for decreased expression levels in the stress groups. **b** Bar plot presenting direction of change in each tRF family. Bar size reflects the number of tRFs in the identified family, with positive values indicating increased levels and negative values indicating decreased levels in the stressed groups. Bar color indicates the significance level, empty bars depict newborns and patterned bars depict mothers. The plot shows the results of males and females together. Sex-separated results are available in Supplementary Tables 3 and 4. Created with BioRender.

male newborns alone revealed a trend of declined expression of Nuc-Asp-i-tRFs (92.9%, FDR = 0.055 in both comparisons). Moreover, comparing the tRF families' profiles between mothers and newborns revealed some cases with opposite trends of change (Fig. 4b), indicating non-random tRF family patterns, which called for seeking possible stress-related interaction between mothers and their newborns.

tRF families show distinct stress-related length distributions

Dicer, Angiogenin, Drosha and other nucleases cleave mature tRNAs to yield the five tRF subtypes (i-tRF, 3′-tRF, etc.), producing various lengths under each cleavage category [20]. To explore tRFs length distributions in our datasets, we calculated the mean levels of all same length tRFs in each newborn cohort (Supplementary Fig. 5a). Both male and female control groups presented non-evenly distributed expression patterns, peaking around the lengths of 23–24 nt, with smaller peaks around 18–19 and 31–32 nt. The highest peak in all groups emerged at the length of 36 nt, but was somewhat attenuated in the female stress group, which showed more even distribution of tRF lengths. Intriguingly, the highest peak in the control groups overlapped known miR lengths, 16–28 nt according to miRbase [57], (Supplementary Fig. 5c). In mothers, we noticed far smaller differences in length distributions between stress and sex groups (Supplementary Fig. 5b), suggesting that newborns' tRFs, more than their mothers, tend to overlap miR lengths, possibly pointing at a shared functional role of targeting and suppressing the expression of mRNAs carrying complementary sequences [23, 87]. Taken together, these findings indicate that mothers' perceived stress may lead to extreme tRFs decline in their newborns' serum.

Next, we tested whether newborn tRFs of particular families tend to appear in specific lengths and are influenced by the mothers' PPS. Using the Kruskal-Wallis test on each tRFs family across the four stress-by-sex groups (Supplementary Fig. 4d)

revealed that numerous newborns' tRF families showed significant preference both towards a single direction of change and a tendency for specific length distributions. Again, the maternal cohort showed no significant length differences between the groups. Notable was the MT-Gln-3′-tRF family, which showed elevated tRF lengths in both control compared to the stress newborn groups, especially in females (Supplementary Fig. 5e, f). Supporting previous reports of stress specificity in tRFs production [20, 22, 27], these findings imply that tRNA cleavage into tRFs is context-specific, presenting stress and sex group differences already at birth.

CholinotRFs and CholinomiRs show specific cholinergic predicted targets

Since tRFs may target genes similarly to miRs and given the cholinergic stress-response network [31, 32], we sought the cholinergic gene targets of the identified tRFs and miRs, combining our in-house scoring system (Fig. 5a) [25–27] with the miRDB target prediction algorithm (22, 23). This identified 13 maternal and 16 newborns "CholinomiRs", showing enrichment compared to those listed in miRbase 22.1 v (Fisher's exact test, maternal and newborn P-values of 0.007 and 0.015, respectively). Additionally, we identified 13 maternal and 38 newborns "CholinotRFs", which were enriched in MT vs. Nuc tRFs in newborns (Fig. 5b; Fisher's exact test, P-value ≤ 0.00001). These values support previous predictions in Parkinson's and Alzheimer's disease [25, 26], deepening the connection of MT-originated tRFs with the cholinergic system under stress and neurodegeneration. Further, the predicted targets identified for the UCS tRFs by miRDB spanned 46% of genes and showed a general enrichment for cholinergic targets (Hypergeometric test, P-value = 0.00015). A wider gene ontology analysis is available in Supplementary Results (Supplementary Fig. 6).

Seeking overlaps between the predicted cholinergic gene targets of CholinomiRs and CholinotRFs in newborns (Fig. 5c, d; Supplementary Tables 6, 7) revealed key cholinergic genes encoding enzymes such as BChE and cytokines like IL6 as targeted by CholinotRFs alone. In contrast, the circadian class of cholinergic genes and most cholinergic receptor genes were co-predicted for targeting by both CholinomiRs and CholinotRFs. However, Spearman correlations between BChE levels in newborns or mothers and its targeting tRFs did not reveal any significant correlations (Supplementary Table 5), a correlation was found between the MT-Gly-i-tRF family and maternal BMI (Supplementary Results). Furthermore, the identified CholinotRFs belonged to 14 MT and three nuclear tRF families. Of those, only seven MT families had more than one CholinotRF member. Specifically, MT-Thr-3′-tRF family four cholinergic members targeted genes across the entire cholinergic landscape, whereas MT-Phe-3′-tRF family four cholinergic members showed specificity toward three cholinergic gene classes. Likewise, the 14 newborn MT CholinotRF families presented specific length distributions, strengthening the notion of stress-driven tRF production.

To validate the predicted targeting quality of the CholinotRFs, we chose the MT-Gly-i-tRF family due to its rise in all the analyses. Of this family, we chose the shortest CholinotRF member (mtDR-36:57-Gly-TCC-1, 21nt long) and used its mimic or scramble sequenced to co-transfected HEK239T cells with a plasmid expressing BCHE or IL6 3′UTR, which the MT-Gly-i-tRF family was predicted to target. We then performed a dual luciferase assay (see Supplementary Methods), showing an average of 31% inhibition for IL6 and 34% for BCHE (Supplementary Fig. 7d).

CholinotRF classify female newborns by their mothers' PPS

To test whether short noncoding RNA levels may classify newborns into stress and control groups, we applied SVM Kernel classification with "leave-one-out" cross-validation to different sets of tRFs and miRs, testing the male and female groups together and apart, and seeking the best group of markers for this task (Supplementary Table 8). Predictably, females presented the best classification, based on the levels of all of the seven UCS DE tRFs and the four female-specific UCS DE tRFs (Fig. 6a), with area under the ROC curve of 100% (AUC; 10,000 permutations, FDR ≤ 0.0001; Supplementary Table 9) and 98%, respectively (FDR = 0.008). Remarkably, the next best classification in female newborns was achieved using the 38 CholinotRFs, yielding AUC of 95% (FDR = 0.008), while CholinomiRs reached an AUC of 88% (FDR = 0.051). Male newborns, however, yielded very low classification scores, all under chance levels (Fig. 6d). When comparing males and females together, testing stress vs. control groups without accounting for sex (Fig. 6b) achieved classification results that were in between those for male and female separately, with the best classification reached using all of the UCS DE tRFs (AUC = 78%, FDR = 0.029). Considering sex as well (Fig. 6c) achieved much better classification, with the lead marker groups still being the UCS DE tRFs (AUC: Female DE tRFs = 94%, FDR = 0.008; all DE tRFs = 93%, FDR = 0.008). Combining our results with the published Fetal stress index (FSI) from the FELICITy cohort, a measurement of fetus heart rate reactivity measured non-invasively during the third trimester [45], elevated some of the classification results, mostly in male newborns (Supplementary Results, Supplementary Fig. 8d-g, Supplementary Table 9), further strengthening the perceived connection of cholinergic tRFs to stress and its sex-specific effects.

DISCUSSION

Maternal PPS has long been known to affect the fetus [5, 8, 11, 12], but validated biomarkers assessing its impact remained lacking. We discovered a new group of biomarkers reflecting maternal PPS impact on the newborn, using tRF expression patterns and ChE catalytic activity levels in maternal and umbilical cord serum. Specifically, we discovered higher AChE activity in the UCS of stressed newborns, with a stronger effect observed in males that indicated cholinergic involvement. This was supported by enriched CholinomiRs and CholinotRFs showing declined levels, with the latter classifying female newborns into stress and control groups with an AUC of 95%.

Importantly, assigning these tRFs to families by their genome origin, cleavage type, and coded amino acid revealed shared expression and length patterns that were specific not only to the differences between mothers and newborns, but also between sex and stress conditions, where female newborns of PPS-affected mothers showed the largest differences.

Our findings have a dual value. First and foremost, we present tRFs as novel biomarkers that differentiated male and female newborns according to maternal stress, assessed at birth. Further, the stress-specific tRF patterns primarily consisted of a major decline of MT tRFs that occurred in both sexes but was more profound in female newborns. Although our cohort is unique, it is small, including only 35 sequenced samples, and due to low RNA quantities, we were not able to validate our findings by qPCR measurements in the rest of the cohort. Furthermore, we did not find publicly available datasets that were similar enough by tissue and species to validate our results, most likely due to the complexity of generating a similar cohort. However, previous animal studies support our observations, specifically in the case of the MT effect: Bartho et al. [88] injected pregnant mice with cortisone between E12.5 and E14.5, which led to a decline in mitochondrial DNA in the placenta of female compared to male offspring; and Su et al. [29] found the overall percentage of MT tRFs in a murine prenatal immune activation model to be higher in the fetal brain and liver of females compared to males. To the best of our knowledge, this effect was not studied in MT-tRNA expression.

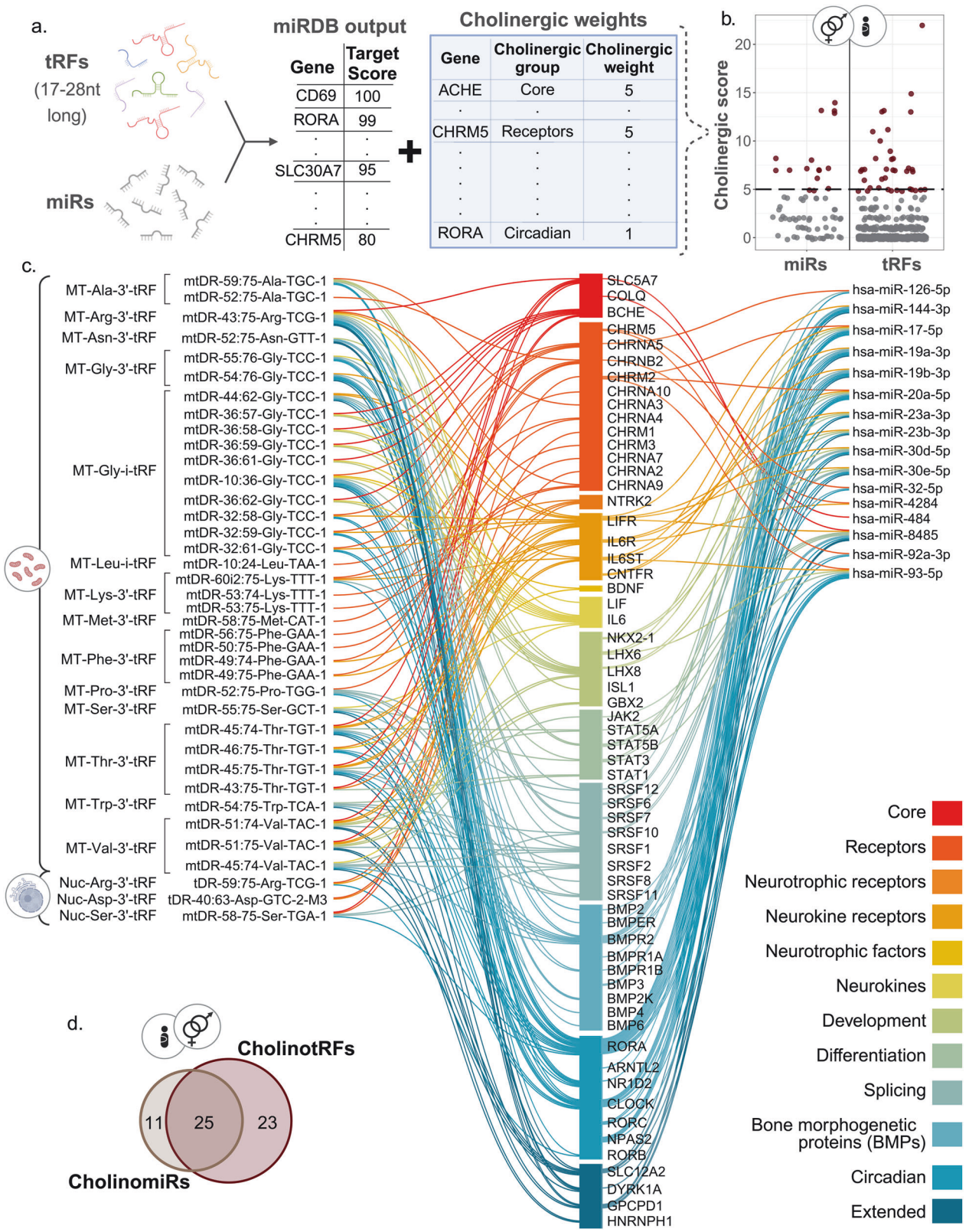

Fig. 5 CholinotRFs and CholinomiRs are predicted to target specific genes in the cholinergic system. a Combining the miRDB sequence-based prediction algorithm with our in-house cholinergic scoring system revealed 16 CholinomiRs and 38 CholinotRFs expressed in newborns. **b** Dot plot showing cholinergic score distribution across UCS miRs and tRFs in both male and female newborns. **c** Network plot presenting predicted targets of the newborn CholinomiRs (right-hand list), and CholinotRFs which are grouped according to their tRF families (left-hand list). tRF families with more than one cholinergic member are framed by black lines. The central list of 51 cholinergic genes that are predicted targets of the CholinomiRs and CholinotRFs is colored according to the class within the cholinergic pathway. **d** Venn plot presenting the number of cholinergic gene targets shared between the newborn CholinomiRs and CholinotRFs. Created with BioRender.

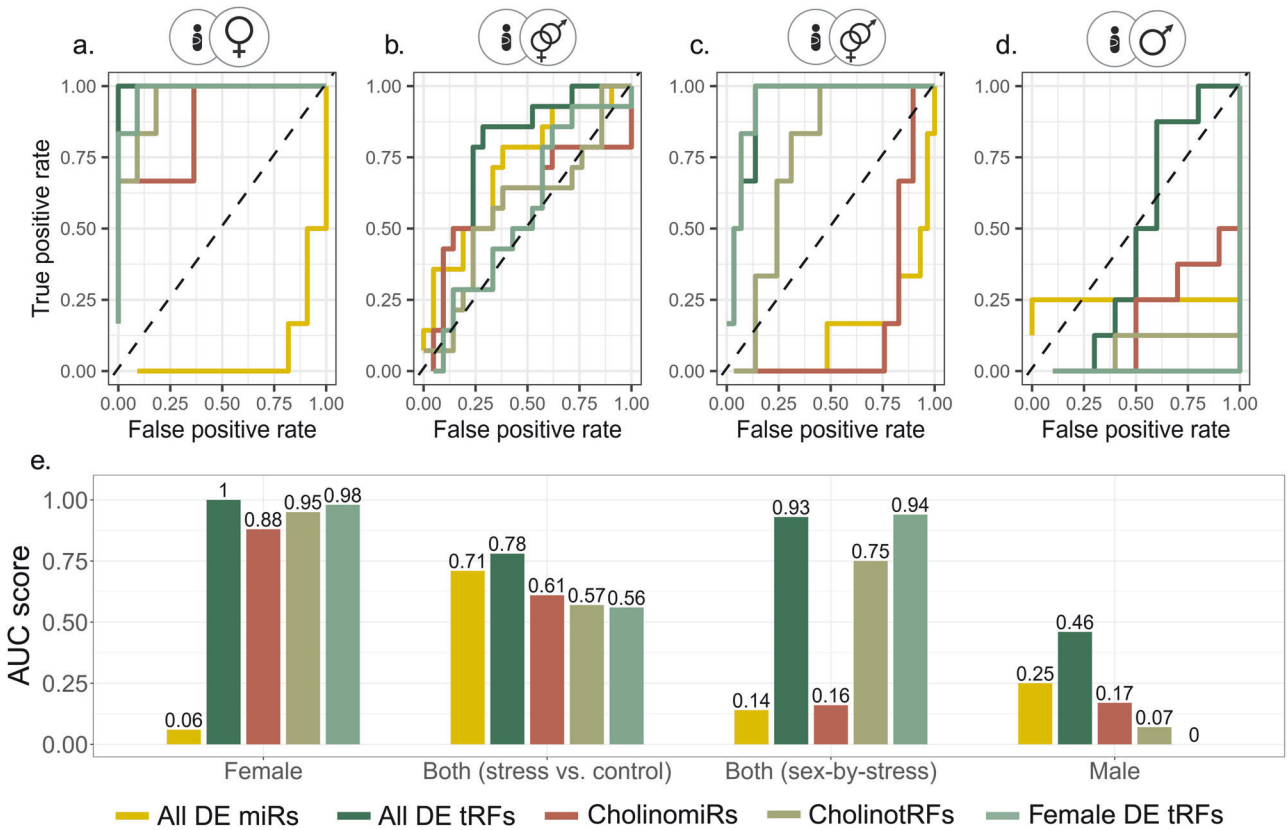

Fig. 6 CholinotRFs classify female newborns according to maternal PPS. a–d ROC curves of five marker groups (All DE tRFs, Female DE tRFs, CholinotRFs, All DE miRs, and CholinomiRs), classifying newborns to stress and control groups based on SVM Kernel algorithm with "leave one out" cross validation: (**a**) females (n = 6 vs. n = 11), (**b**) males & females (stress vs. control; n = 14 vs. n = 21), (**c**) males & females (stress-by-sex; n = 14 vs. n = 21), and (**d**) males (n = 8 vs. n = 10). **e** Bar plot of AUC values across comparisons with FDR based on 10,000 permutations (available in Supplementary table 9). Created with BioRender.

The magnitude of the MT tRF effect can also reflect the use of serum rather than whole blood or PBMCs. Serum RNA reflects the extracellular vesicles and broken blood cells content, including platelets which are rich in mitochondria [89]. While serum RNA amounts are low [90], which requires more specialized library preparation kits, the enrichment in short RNAs compensates for the low yield [90, 91]. Further, serum is the standard blood fraction in use in hospital settings and therefore forms an available pool for RNA-seq clinical studies.

Serum is also a standard tissue for measuring cholinergic tone, defined as the balance between AChE and BChE, both of which hydrolyze acetylcholine to acetate and choline. AChE acts as the main cholinesterase of the central nervous system and BChE of the periphery [31, 32]. In the fetal environment, besides the erythrocyte-bound blood AChE [37], AChE is found in the placenta and in umbilical cord endothelial cells [38, 39]. Indeed, we found higher AChE levels in the UCS compared to the maternal serum, followed by stress-related elevation in newborns. This effect was more predominant in male compared to female newborns, compatible with reports of larger stress-related differences in male newborns [5, 14, 44]. By hydrolyzing acetylcholine, the two ChEs can suppress its anti-inflammatory effect, activating pro-inflammatory pathways including the NF-κB pathway which contradicts the vagus-mediated acetylcholine secretion in response to an activated HPA [32–34, 92]. The regulation of this cascade by short noncoding RNAs [37, 92] echoes our findings of the seemingly unrelated enriched CholinotRFs and CholinomiRs and the two ChEs in our data. Furthermore, transgenic excess of the AChE-targeting CholinomiR miR-132 was incompatible with fetal survival in mice [93]; also, cholinesterase enzymes in male mice were directly influenced by prenatal physical and psychological stress, and hyperexcitability of the cholinergic neurons in the latero-dorsal tegmentum may cause anxiety-like behaviors and memory impairment [94].

Secondly, and as important, is our novel interpretation of tRF sequencing results. Although sets of tRFs share many characteristics that warrant their assembly into groups, they are still perceived by the scientific community as separate entities. Thus, while the literature often mentions tRFs by their "family name" (MT itRF^{HisGTG}, Glu-50tsRNA-CTC, etc.) [95, 96], they are still referred to as single tRF molecules. In contradistinction, our classification into "tRF families" based on a combination of their genome origin, cleavage type and coded amino acid, has highlighted expression and length patterns that are context-specific, i.e., influenced by stress and sex. Furthermore, previous studies have identified "tRF storms", characterized by rising levels of tRFs that replaced miRs two days post-stroke [27]. Indeed, in our data we saw that these family patterns passed the boundary of single parental tRNA gene and were shared even between all of the tRFs of the same coded amino acid. This marks the importance of mass production of tRFs [22] and strengthens the concept that tRFs function as groups rather than as individuals.

To the best of our knowledge, reference to tRF groups appeared in partial ways in three previous studies. The most recent, by Akins et al. [97], examined multiple datasets seeking 5′-halfs and long 5′-tRFs in human patients and cell lines. They showed that while context-dependent, tRFs that share length and parental tRNA may also share expression levels and sequence. However, their DE analysis did not examine tRF families as groups directly, and their focus was on 5′ -tRFs and -halves of specific lengths, 27–41 nt,

which were almost completely absent in our data. Su et al. [29] investigated the influence of prenatal maternal immune activation in mice on tRFs in several tissues. Immune activation was performed at E11.5 and E12.5 and within a few hours after the second activation they thoroughly investigated the tRF landscape, including an in-depth characterization of the length distribution according to cleavage type by both sequencing and northern blot analyses of tRFs grouped by their parental tRNAs. However, using STAR alignment [98] rather than the standard annotations of tRFs, rendered their analysis less translatable by the standard tools of the field. The third study, by Isakova et al. [99], aligned tRFs with a combination of STAR and Unitas [100] too, as one part of a complex atlas of short noncoding RNAs in different murine tissues. Grouping tRFs based on their genome origin, cleavage type, and coded amino acid codon, showed tissue-specific expression patterns, however, their only statistic for assessing tRFs as groups was the sum of expression, overlooking the variability within said groups. Further, i-tRFs were absent from their analysis.

Finally, all three papers retained groupings based on single amino acid codons, while we have shown that similar expression patterns were shared even within the wider boundaries of a single amino acid coded by several codons. Our introduction of the binomial test allowed for the quantitative examination of how tRF families function as groups, by testing shared expression patterns, length distributions and sequence similarities. Nevertheless, we wish to stress out the importance of previous reports establishing specific functions of single tRFs in diverse diseases and conditions [23, 25–28, 30], and urge future researchers to take these points into account and seek both single and familial tRF functions.

In conclusion, we have shown the involvement of PPS in affecting the cholinergic system at diverse levels, by modulating newborns ChE activities, CholinomiRs and CholinotRFs. Our study demonstrated the importance of tRF families as sex-specific biomarkers that reflect the effect of maternal PPS on newborns, as early as the birth itself. We presented a new analysis approach that considers the group function of tRFs as families, as determined by their genome origin, cleavage type, and coded amino acid, rather than as single tRFs. We believe that these findings play an important role in the early diagnosis of stress effects in newborns and encourage further research into the landscape of tRFs in prenatal and other stress-related conditions.

DATA AVAILABILITY

The sequencing data underlying this article can be found under accession GSE275149 in the GEO website.

REFERENCES

1. Bakhireva LN, Solomon E, Roberts MH, Ma X, Rai R, Wiesel A, et al. Independent and combined effects of prenatal alcohol exposure and prenatal stress on fetal HPA axis development. Int J Mol Sci. 2024;25:2690.
2. Muglia LJ, Benhalima K, Tong S, Ozanne S. Maternal factors during pregnancy influencing maternal, fetal, and childhood outcomes. BMC Med. 2022;20:418.
3. Kumar D, Verma S, Mysorekar IU. COVID-19 and pregnancy: clinical outcomes; mechanisms, and vaccine efficacy. Transl Res. 2023;251:84–95.
4. Wu Y, Espinosa KM, Barnett SD, Kapse A, Quistorff JL, Lopez C, et al. Association of elevated maternal psychological distress, altered fetal brain, and offspring cognitive and social-emotional outcomes at 18 months. JAMA Netw Open. 2022;5:e229244.
5. Walsh K, McCormack CA, Webster R, Pinto A, Lee S, Feng T, et al. Maternal prenatal stress phenotypes associate with fetal neurodevelopment and birth outcomes. Proc Natl Acad Sci. 2019;116:23996–4005.
6. Schalla MA, Stengel A. The role of stress in perinatal depression and anxiety – a systematic review. Front Neuroendocrinol. 2024;72:101117.
7. Cohen S, Kamarck T, Mermelstein R. A global measure of perceived stress. J Health Soc Behav. 1983;24:385.
8. Graham AM, Doyle O, Tilden EL, Sullivan EL, Gustafsson HC, Marr M, et al. Effects of maternal psychological stress during pregnancy on offspring brain development: considering the role of inflammation and potential for preventive intervention. Biol Psychiatry Cogn Neurosci Neuroimaging. 2022;7:461–70.
9. Van den Bergh BRH, Antonelli MC, Stein DJ. Current perspectives on perinatal mental health and neurobehavioral development: focus on regulation, coregulation and self-regulation. Curr Opin Psychiatry. 2024;37:237–50.
10. Wu Y, Lu Y-C, Jacobs M, Pradhan S, Kapse K, Zhao L, et al. Association of prenatal maternal psychological distress with fetal brain growth, metabolism, and cortical maturation. JAMA Netw Open. 2020;3:e1919940.
11. Moog NK, Nolvi S, Kleih TS, Styner M, Gilmore JH, Rasmussen JM, et al. Prospective association of maternal psychosocial stress in pregnancy with newborn hippocampal volume and implications for infant social-emotional development. Neurobiol Stress. 2021;15:100368.
12. Moshfeghinia R, Torabi A, Mostafavi S, Rahbar S, Moradi MS, Sadeghi E, et al. Maternal psychological stress during pregnancy and newborn telomere length: a systematic review and meta-analysis. BMC Psychiatry. 2023;23:947.
13. Entringer S, Epel ES, Lin J, Buss C, Shahbaba B, Blackburn EH, et al. Maternal psychosocial stress during pregnancy is associated with newborn leukocyte telomere length. Am J Obstet Gynecol. 2013;208:134.e1–134.e7.
14. Lehtola SJ, Tuulari JJ, Scheinin NM, Karlsson L, Parkkola R, Merisaari H, et al. Newborn amygdalar volumes are associated with maternal prenatal psychological distress in a sex-dependent way. Neuroimage Clin. 2020;28:102380.
15. Cao-Lei L, de Rooij SR, King S, Matthews SG, Metz GAS, Roseboom TJ, et al. Prenatal stress and epigenetics. Neurosci Biobehav Rev. 2020;117:198–210.
16. Hantsoo L, Kornfield S, Anguera MC, Epperson CN. Inflammation: a proposed intermediary between maternal stress and offspring neuropsychiatric risk. Biol Psychiatry. 2019;85:97–106.
17. Vuppaladhadiam L, Lager J, Fiehn O, Weiss S, Chesney M, Hasdemir B, et al. Human placenta buffers the fetus from adverse effects of perceived maternal stress. Cells. 2021;10:379.
18. Chen Q, Zhang X, Shi J, Yan M, Zhou T. Origins and evolving functionalities of tRNA-derived small RNAs. Trends Biochem Sci. 2021;46:790–804.
19. Kuhle B, Chen Q, Schimmel P. tRNA renovatio: rebirth through fragmentation. Mol Cell. 2023;83:3953–71.
20. Magee R, Rigoutsos I. On the expanding roles of tRNA fragments in modulating cell behavior. Nucleic Acids Res. 2020;48:9433–48.
21. Telonis AG, Kirino Y, Rigoutsos I. Mitochondrial tRNA-lookalikes in nuclear chromosomes: could they be functional? RNA Biol. 2015;12:375–80.
22. Yu X, Xie Y, Zhang S, Song X, Xiao B, Yan Z. tRNA-derived fragments: mechanisms underlying their regulation of gene expression and potential applications as therapeutic targets in cancers and virus infections. Theranostics. 2021;11:461–9.
23. Fu M, Gu J, Wang M, Zhang J, Chen Y, Jiang P, et al. Emerging roles of tRNA-derived fragments in cancer. Mol Cancer. 2023;22:30.
24. Su Z, Wilson B, Kumar P, Dutta A. Noncanonical roles of tRNAs: tRNA fragments and beyond. Annu Rev Genet. 2020;54:47–69.
25. Shulman D, Dubnov S, Zorbaz T, Madrer N, Paldor I, Bennett DA, et al. Sex-specific declines in cholinergic-targeting tRNA fragments in the nucleus accumbens in Alzheimer's disease. Alzheimer's Dement. 2023;19:5159–72.
26. Paldor I, Madrer N, Vaknine Treidel S, Shulman D, Greenberg DS, Soreq H Cerebrospinal fluid and blood profiles of transfer RNA fragments show age, sex, and Parkinson's disease-related changes. J Neurochem. 2022. https://doi.org/10.1111/jnc.15723.
27. Winek K, Lobentanzer S, Nadorp B, Dubnov S, Dames C, Jagdmann S, et al. Transfer RNA fragments replace microRNA regulators of the cholinergic poststroke immune blockade. Proc Natl Acad Sci USA. 2020;117:32606–16.
28. Tzur Y, Winek K, Madrer N, Dubnov S, Bennett ER, Greenberg DS, et al. Lysine tRNA fragments and miR-194-5p co-regulate hepatic steatosis via β-Klotho and perilipin 2. Mol Metab. 2024;79:101856.
29. Su Z, Frost EL, Lammert CR, Przanowska RK, Lukens JR, Dutta A. tRNA-derived fragments and microRNAs in the maternal-fetal interface of a mouse maternal-immune-activation autism model. RNA Biol. 2020;17:1183–95.
30. Cooke WR, Jiang P, Ji L, Bai J, Jones GD, Lo YMD, et al. Differential 5′-tRNA fragment expression in circulating preeclampsia syncytiotrophoblast vesicles drives macrophage inflammation. Hypertension. 2024;81:876–86.
31. Soreq H. Checks and balances on cholinergic signaling in brain and body function. Trends Neurosci. 2015;38:448–58.
32. Vaknine S, Soreq H. Central and peripheral anti-inflammatory effects of acetylcholinesterase inhibitors. Neuropharmacology. 2020;168:108020.
33. Cerritelli F, Frasch MG, Antonelli MC, Viglione C, Vecchi S, Chiera M, et al. A review on the vagus nerve and autonomic nervous system during fetal development: searching for critical windows. Front Neurosci. 2021;15:1184.
34. Chavan SS, Pavlov VA, Tracey KJ. Mechanisms and therapeutic relevance of neuro-immune communication. Immunity. 2017;46:927–42.

35. Shenhar-Tsarfaty S, Berliner S, Bornstein NM, Soreq H. Cholinesterases as biomarkers for parasympathetic dysfunction and inflammation-related disease. J Mol Neurosci. 2014;53:298–305.
36. Winek K, Soreq H, Meisel A. Regulators of cholinergic signaling in disorders of the central nervous system. J Neurochem. 2021;158:1425–38.
37. Madrer N, Soreq H. Cholino-ncRNAs modulate sex-specific- and age-related acetylcholine signals. FEBS Lett. 2020;594:2185–98.
38. Carvalho AF, Graça LM, Martins-Silva J, Saldanha C. Biochemical characterization of human umbilical vein endothelial cell membrane bound acetylcholinesterase. FEBS J. 2005;272:5584–94.
39. Ruma Sun-y BV. Human placentai cholinergic system. Biochem Pharmacol. 1997;53:1577–86.
40. Nadorp B, Soreq H. Predicted overlapping microRNA regulators of acetylcholine packaging and degradation in neuroinflammation-related disorders. Front Mol Neurosci. 2014;7:9.
41. Lobentanzer S, Hanin G, Klein J, Soreq H. Integrative transcriptomics reveals sexually dimorphic control of the cholinergic/neurokine interface in schizophrenia and bipolar disorder. Cell Rep. 2019;29:764–77.e5.
42. Antonelli MC, Frasch MG, Rumi M, Sharma R, Zimmermann P, Molinet MS, et al. Early biomarkers and intervention programs for the infant exposed to prenatal stress. Curr Neuropharmacol. 2022;20:94–106.
43. Sharma R, Frasch MG, Zelgert C, Zimmermann P, Fabre B, Wilson R, et al. Maternal–fetal stress and DNA methylation signatures in neonatal saliva: an epigenome-wide association study. Clin Epigenetics. 2022;14:87.
44. Zimmermann P, Antonelli MC, Sharma R, Müller A, Zelgert C, Fabre B, et al. Prenatal stress perturbs fetal iron homeostasis in a sex specific manner. Sci Rep. 2022;12:9341.
45. Lobmaier SM, Müller A, Zelgert C, Shen C, Su PC, Schmidt G, et al. Fetal heart rate variability responsiveness to maternal stress, non-invasively detected from maternal transabdominal ECG. Arch Gynecol Obstet. 2020;301:405–14.
46. Alderdice F, Lynn F. Factor structure of the prenatal distress questionnaire. Midwifery. 2011;27:553–9.
47. Ellman GL, Courtney KD, Andres V, Featherstone RM. A new and rapid colorimetric determination of acetylcholinesterase activity. Biochem Pharmacol. 1961;7:88–95.
48. R Core Team. R: a language and environment for statistical computing. 2019. https://www.r-project.org/.
49. Pös O, Biró O, Szemes T, Nagy B. Circulating cell-free nucleic acids: characteristics and applications. Eur J Hum Genet. 2018;26:937–45.
50. Andrews S. FastQC a quality control tool for high throughput sequence data. 2010. https://www.bioinformatics.babraham.ac.uk/projects/fastqc/.
51. Martin M. Cutadapt removes adapter sequences from high-throughput sequencing reads. EMBnet J. 2011;17:10–12.
52. Dodt M, Roehr JT, Ahmed R, Dieterich C. FLEXBAR-flexible barcode and adapter processing for next-generation sequencing platforms. Biology. 2012;1:895–905.
53. Roehr JT, Dieterich C, Reinert K. Flexbar 3.0 - SIMD and multicore parallelization. Bioinformatics. 2017;33:2941–2.
54. Loher P, Telonis AG, Rigoutsos I. MINTmap: fast and exhaustive profiling of nuclear and mitochondrial tRNA fragments from short RNA-seq data. Sci Rep. 2017;7:41184.
55. Pliatsika V, Loher P, Telonis AG, Rigoutsos I. MINTbase: a framework for the interactive exploration of mitochondrial and nuclear tRNA fragments. Bioinformatics. 2016;32:2481–9.
56. Friedländer MR, MacKowiak SD, Li N, Chen W, Rajewsky N. MiRDeep2 accurately identifies known and hundreds of novel microRNA genes in seven animal clades. Nucleic Acids Res. 2012;40:37–52.
57. Kozomara A, Birgaoanu M, Griffiths-Jones S. miRBase: from microRNA sequences to function. Nucleic Acids Res. 2019;47:D155–D162.
58. Griffiths-Jones S, Saini HK, van Dongen S, Enright AJ. miRBase: tools for microRNA genomics. Nucleic Acids Res. 2007;36:D154–D158.
59. Holmes AD, Chan PP, Chen Q, Ivanov P, Drouard L, Polacek N, et al. A standardized ontology for naming tRNA-derived RNAs based on molecular origin. Nat Methods. 2023;20:627–8.
60. Love MI, Huber W, Anders S. Moderated estimation of fold change and dispersion for RNA-seq data with DESeq2. Genome Biol. 2014;15:1–21.
61. Liu W, Wang X. Prediction of functional microRNA targets by integrative modeling of microRNA binding and target expression data. Genome Biol. 2019;20:1–10.
62. Chen Y, Wang X. miRDB: an online database for prediction of functional microRNA targets. Nucleic Acids Res. 2020;48:D127–D131.
63. Kuhn M. caret: Classification and Regression Training. 2022. https://CRAN.R-project.org/package=caret.
64. John C R. MLeval: Machine Learning Model Evaluation. 2020. https://cran.r-project.org/web/packages/MLeval/index.html.
65. Vlachos DG, Schulpis KH, Parthimos T, Mesogitis S, Vlachos GD, Partsinevelos GA, et al. The effect of the mode of delivery on the maternal-neonatal erythrocyte membrane acetylcholinesterase activity. Clin Biochem. 2008;41:818–23.
66. Selmaj I, Cichalewska M, Namiecinska M, Galazka G, Horzelski W, Selmaj KW, et al. Global exosome transcriptome profiling reveals biomarkers for multiple sclerosis. Ann Neurol. 2017;81:703–17.
67. Barnett MM, Reay WR, Geaghan MP, Kiltschewskij DJ, Green MJ, Weidenhofer J, et al. miRNA cargo in circulating vesicles from neurons is altered in individuals with schizophrenia and associated with severe disease. Sci Adv. 2023;9:eadi4386.
68. Håvik B, Le Hellard S, Rietschel M, Lybæk H, Djurovic S, Mattheisen M, et al. The complement control-related genes CSMD1 and CSMD2 associate to schizophrenia. Biol Psychiatry. 2011;70:35–42.
69. Liu Y, Fu X, Tang Z, Li C, Xu Y, Zhang F, et al. Altered expression of the CSMD1 gene in the peripheral blood of schizophrenia patients. BMC Psychiatry. 2019;19:113.
70. Flamant S, Chomel JC, Desterke C, Féraud O, Gobbo E, Mitjavila-Garcia MT, et al. Global microRNA profiling uncovers miR-206 as a negative regulator of hematopoietic commitment in human pluripotent stem cells. Int J Mol Sci. 2019;20:1737.
71. Mikulski D, Nowicki M, Dróżdż I, Misiewicz M, Kościelny KP, Okoński K, et al. High serum miR-223-3p expression level predicts complete response and prolonged overall survival in multiple myeloma patients undergoing autologous hematopoietic stem cell transplantation. Front Oncol. 2023;13:1250355.
72. Su S, Zhao Q, He C, Huang D, Liu J, Chen F, et al. miR-142-5p and miR-130a-3p are regulated by IL-4 and IL-13 and control profibrogenic macrophage program. Nat Commun. 2015;6:8523.
73. Liao R, Sun J, Zhang L, Lou G, Chen M, Zhou D, et al. MicroRNAs play a role in the development of human hematopoietic stem cells. J Cell Biochem. 2008;104:805–17.
74. Kim BS, Jung JY, Jeon JY, Kim HA, Suh CH. Circulating hsa-miR-30e-5p, hsa-miR-92a-3p, and hsa-miR-223-3p may be novel biomarkers in systemic lupus erythematosus. HLA. 2016;88:187–93.
75. Ma F, Chen D, Chi Y, Chen F, Li X, Han Z. The expression and role of miR-301a in human umbilical cord-derived mesenchymal stromal cells. Cytotherapy. 2013;15:1511–6.
76. Granda-Díaz R, Manterola L, Hermida-Prado F, Rodríguez R, Santos L, García-de-la-Fuente V, et al. Targeting oncogenic functions of miR-301a in head and neck squamous cell carcinoma by PI3K/PTEN and MEK/ERK pathways. Biomed Pharmacother. 2023;161:114512.
77. Fernández-Pato A, Virseda-Berdices A, Resino S, Ryan P, Martínez-González O, Pérez-García F, et al. Plasma miRNA profile at COVID-19 onset predicts severity status and mortality. Emerg Microbes Infect. 2022;11:676–88.
78. Seong RK, Lee JK, Cho GJ, Kumar M, Shin OS. mRNA and miRNA profiling of Zika virus-infected human umbilical cord mesenchymal stem cells identifies miR-142-5p as an antiviral factor. Emerg Microbes Infect. 2020;9:2061–75.
79. Hamza S, Garanina EE, Shkair L, Alsaadi M, Khaiboullina SF, Tezcan G. Implications of NLRP3 suppression using glibenclamide and miR-223 against colorectal cancer. Pharmaceuticals. 2024;17:299.
80. Stverakova T, Baranova I, Mikyskova P, Gajdosova B, Vosmikova H, Laco J, et al. Selection of endogenous control and identification of significant microRNA deregulations in cervical cancer. Front Oncol. 2023;13:1143691.
81. Zhang X, Yan Z, Zhang J, Gong L, Li W, Cui J, et al. Combination of hsa-miR-375 and hsa-miR-142-5p as a predictor for recurrence risk in gastric cancer patients following surgical resection. Ann Oncol. 2011;22:2257–66.
82. Pillay P, Moodley K, Vatish M, Moodley J. Exosomal microRNAs in pregnancy provides insight into a possible cure for cancer. Int J Mol Sci. 2020;21:1–16.
83. Gu H, Chen L, Xue J, Huang T, Wei X, Liu D, et al. Expression profile of maternal circulating microRNAs as non-invasive biomarkers for prenatal diagnosis of congenital heart defects. Biomed Pharmacother. 2019;109:823–30.
84. Chan PP, Lowe TM. GtRNAdb: a database of transfer RNA genes detected in genomic sequence. Nucleic Acids Res. 2009;37:93–97.
85. Chan PP, Lowe TM. GtRNAdb 2.0: an expanded database of transfer RNA genes identified in complete and draft genomes. Nucleic Acids Res. 2016;44:D184–D189.
86. Juhling F, Morl M, Hartmann RK, Sprinzl M, Stadler PF, Putz J. tRNAdb 2009: compilation of tRNA sequences and tRNA genes. Nucleic Acids Res. 2009;37:D159–D162.
87. Blaze J, Akbarian S. The tRNA regulome in neurodevelopmental and neuropsychiatric disease. Mol Psychiatry. 2022;27:3204–13.
88. Bartho LA, Holland OJ, Moritz KM, Perkins AV, Cuffe JSM. Maternal corticosterone in the mouse alters oxidative stress markers, antioxidant function and mitochondrial content in placentas of female fetuses. J Physiol. 2019;597:3053–67.
89. Picard M. Blood mitochondrial DNA copy number: What are we counting? Mitochondrion. 2021;60:1–11.

90. Hulstaert E, Morlion A, Avila Cobos F, Verniers K, Nuytens J, Vanden Eynde E, et al. Charting extracellular transcriptomes in the human biofluid RNA atlas. Cell Rep. 2020;33:108552.
91. Godoy PM, Bhakta NR, Barczak AJ, Cakmak H, Fisher S, MacKenzie TC, et al. Large differences in small RNA composition between human biofluids. Cell Rep. 2018;25:1346–58.
92. Zorbaz T, Madrer N, Soreq H. Cholinergic blockade of neuroinflammation: from tissue to RNA regulators. Neuronal Signal. 2022;6:NS20210035.
93. Hanin G, Yayon N, Tzur Y, Haviv R, Bennett ER, Udi S, et al. miRNA-132 induces hepatic steatosis and hyperlipidaemia by synergistic multitarget suppression. Gut. 2018;67:1124–34.
94. Shabani M, Ilaghi M, Naderi R, Razavinasab M. The hyperexcitability of later-odorsal tegmentum cholinergic neurons accompanies adverse behavioral and cognitive outcomes of prenatal stress. Sci Rep. 2023;13:6011.
95. Soureas K, Papadimitriou M, Malandrakis P, Papanota A, Adamopoulos PG, Ntanasis-Stathopoulos I, et al. Small RNA-seq and clinical evaluation of tRNA-derived fragments in multiple myeloma: loss of mitochondrial i-tRF HisGTG results in patients' poor treatment outcome. Br J Haematol. 2024;204:1790–1800. https://doi.org/10.1111/bjh.19332
96. Li D, Gao X, Ma X, Wang M, Cheng C, Xue T, et al. Aging-induced tRNAGlu-derived fragment impairs glutamate biosynthesis by targeting mitochondrial translation-dependent cristae organization. Cell Metab. 2024;36:1059–75.e9. https://doi.org/10.1016/j.cmet.2024.02.011
97. Akins RB, Ostberg K, Cherlin T, Tsiouplis NJ, Loher P, Rigoutsos I. The typical tRNA Co-expresses multiple 5′ tRNA halves whose sequences and abundances depend on isodecoder and isoacceptor and change with tissue type, cell Type, and disease. Noncoding RNA. 2023;9:69.
98. Dobin A, Davis CA, Schlesinger F, Drenkow J, Zaleski C, Jha S, et al. STAR: ultrafast universal RNA-seq aligner. Bioinformatics. 2013;29:15–21.
99. Isakova A, Fehlmann T, Keller A, Quake SR. A mouse tissue atlas of small non-coding RNA. Proc Natl Acad Sci USA. 2020;117:25634–45. https://doi.org/10.1073/pnas.2002277117/-/DCSupplemental
100. Gebert D, Hewel C, Rosenkranz D. Unitas: the universal tool for annotation of small RNAs. BMC Genomics. 2017;18:644.

ACKNOWLEDGEMENTS

The authors wish to thank all participants and all the medical staff at the labor and delivery teams of the Department of Obstetrics and Gynecology (Klinikum rechts der Isar, Technical University of Munich, Germany) for their valuable contribution to the study. The research leading to these results received funding from the Israel Science Foundation, ISF (835/23; to H.S.), the European Research Council (Advanced Award 321501, to H.S.), and from a joint research support to H.S. and L.C. from The Hebrew University. We further acknowledge the Ken Stein foundation's support. L.C. is the Snyder Granadar chair in Genetics, H.S. is the Slesinger chair in Molecular Neuroscience. This work was further supported by a Hans Fischer Senior Fellowship from IAS-TUM (Institute for Advanced Study - Technical University of Munich, Munich, Germany) awarded to M.C.A., as well as funds from the Department of Obstetrics and Gynecology, Klinikum rechts der Isar, Technical University of Munich, Germany to S.M.L., and CIHR to M.G.F. (grant number 123489). Finally, we wish to thank Patricia P. Chan and the tDRnamer team for their kind help providing us with an MT-addition to their algorithm.

AUTHOR CONTRIBUTIONS

SVT conducted experiments, managed and performed data analysis, and drafted the manuscript. SML, MCA, and MGF performed data collection management and edited the manuscript. RS, PG, and AT participated in running experiments. CZ and PZ recruited the participants, and collected samples and demographic data. NM, SD, and DS contributed to data analysis. ERB helped design and run experiments, and participated in manuscript writing and editing. DSG helped in manuscript writing and editing. LC provided guidance on statistical and data analyses, and helped write and edit the manuscript. HS managed the project and manuscript writing and editing.

FUNDING

Open access funding provided by Hebrew University of Jerusalem.

COMPETING INTERESTS

The authors declare no competing interests.

ETHICS APPROVAL

The study protocol is in strict accordance with the Committee of Ethical Principles for Medical Research from TUM and has the approval of the 'Ethikkommission der Fakultat fur Medizin der Technische Universitat Munchen' (registration number 151/16S). ClinicalTrials.gov registration number is NCT03389178. Written informed consent was received from participants prior to inclusion in the study. All methods were performed in accordance with the relevant guidelines and regulations.

ADDITIONAL INFORMATION

Supplementary information The online version contains supplementary material available at https://doi.org/10.1038/s41380-025-03011-2.

Correspondence and requests for materials should be addressed to Hermona Soreq.

Reprints and permission information is available at http://www.nature.com/reprints

Publisher's note Springer Nature remains neutral with regard to jurisdictional claims in published maps and institutional affiliations.